

DIFFRACTION EFFECTS IN A SOUND BEAM PROPAGATING THROUGH A NON-UNIFORM FLOWING FLUID

D Tchatat
Ngaha Department of Computer Science, Electrical Engineering and Mathematical Sciences, Western Norway University of Applied Sciences, 5063 Bergen, Norway

K-E Frøysa Department of Computer Science, Electrical Engineering and Mathematical Sciences, Western Norway University of Applied Sciences, 5063 Bergen, Norway

1 INTRODUCTION

In pipe flow of natural gas, the flow velocity can be up to 40 m/s or exceeding a bit, corresponding to about 10% of the speed of sound.

In order to study how such a large flow affects a sound beam in the case where the flow direction is perpendicular to the acoustic beam, a parabolic equation is used^{1,2,3}. The acoustic beam is generated by a uniform piston source. It is demonstrated that the acoustic beam will be bent significantly, and this effect should be taken into account when using such an acoustic beam for example for determination of flow velocity^{2,3}.

For pipe flow of oil, the flow velocity is lower and the speed of sound larger. This means that the flow velocity is about 1% of the speed of sound or lower. In this case, the flow effects on the acoustic beam are smaller.

In the present paper it is investigated whether such a beam-flow interaction can be important to take into account also for underwater acoustics. It is focused on small range propagations, up to about 10 metres. Ocean currents are often in the range about 1 m/s. For generality, current velocities up to 5 m/s have been considered. Flow effects on the amplitude and phase are investigated. Applications of this study may be e.g. within echosounders and acoustic positioning systems. Within the limitations of this study, it is shown that the effects of alteration of the acoustic beam by flow is minor, and in most cases can be neglected.

2 THEORY

Sound waves radiating in moving fluid over a small range distance can refer to the study of how sound waves travel and interact in medium such as natural gas or water. The accuracy of the acoustic wave propagating in a flowing fluid depends on many factors, including the flow velocity distribution of the fluid over a propagation distance. But often, this accuracy is subject to numerous challenges such as flow effects or flow disturbances and diffraction effects. In pipe flow, various techniques have been investigated to

reduce and overcome the effects of such factors on sound propagation, such as using specialized sound sources and signal processing algorithms, the positioning of flow conditioner designs in the pipeline, or the use of piston diffraction correction models^{5,6,7}, to name a few.

However, in underwater acoustic applications, when sound waves travel through water, the sound field can be affected by various factors such as temperature, salinity, pressure, and the presence of obstacles or boundaries^{8,9,11}. Even over short distances, factors such as absorption, refraction, diffraction, scattering and noise or variations in the sound field due to changes in the flow velocity and direction can result in changes in the intensity and direction of the sound waves, leading to variations in the way the waves propagate and interact with the surrounding environment^{10,11}. In this work, a combination of diffraction and flow effects is studied.

Thus, flow-acoustic coupling are worth for this study, and in the broad sense it requires a well developed model that can describe such interactions. However, here a simplified set-up of some inputs in underwater acoustic, such as the acoustics path, beam angle, sound source, the distribution of velocities in the axial direction over the propagation distance, are defined to reflect gradually underwater acoustics over a short distance. Motivated by ultrasonic sound fields in open water, some other assumptions relying on the underwater acoustic process are set as follows:

- i. The sound source is a uniform piston located in a flat baffle, located at $z = 0$ radiating only into the half-space $z > 0$. No bottom and surface reflections or additive noise from other sources than the piston source itself are considered.
- ii. For the purpose of comparing and highlighting the flow effects on acoustic waves between different flow profiles, we consider a laminar flow profile because we have that model in Ngaha et al.^{3,4}. Even though this laminar flow is not 100% realistic, it is used and compared to the uniform flow profile in Ngaha et al.^{1,2}. For this reason, the fluid is considered to be homogeneous (speed of sound and ambient density are independent of space $\mathbf{x} = (x, y, z)$ and time t). Water currents flow in the x -direction, considered as a laminar flow of velocity $v_{0x} = v_{x,max} \left(1 - \frac{(z-r)^2}{r^2}\right)$ when $0 \leq z \leq z_{max}$, with z_{max} being the maximal transducer axis and $v_{x,max}$ (constant) is maximum flow velocity at the centerline at $r = z_{max}/2$. The water current is in a direction perpendicular to the acoustical axis of the transmitting ultrasonic transducer. For the uniform flow profile, the flow velocity is $v_{0x} = v_{x,max}$. The flow is also here in the x -direction and is thus perpendicular to the acoustical axis of the transmitting ultrasonic transducer.
- iii. No effective speed of sound is considered due to the choice of flow direction. Neither acoustic refractive index in the flowing water is assessed due to the homogeneity of the fluid.

Several equations relying on sound waves in flowing fluids can deal with the assumptions above in various set such as the Helmholtz-type equations of sound fields through a moving medium by Pierce¹² and Ostashev et al.¹³. But those equations are exhausting in computation and as we deal with underwater acoustic over a small distance, a high-frequency, narrow-angle three-dimensional parabolic equation as found in (Eq. 2.111, Ostashev et al.¹³) is used, and based on assumptions above, it is reduced to

$$\frac{\partial^2 q}{\partial x^2}(\mathbf{x}) + \frac{\partial^2 q}{\partial y^2}(\mathbf{x}) + 2\frac{ik}{c}v_{0x}(z)\frac{\partial q}{\partial x}(\mathbf{x}) + 2ik\frac{\partial q}{\partial z}(\mathbf{x}) = 0. \quad (1)$$

The boundary condition at $z = 0$ is expressed as $q(x, y, 0) = \rho_0 c \bar{v}_s$ when $x^2 + y^2 < a^2$ (B), and 0 elsewhere, where the sound pressure is $P(\mathbf{x}, t) = \text{Re}\{e^{i(kz - \omega t)} q(\mathbf{x})\}$. a (constant) is the sound source radius, c is the speed of sound in the medium, ρ_0 is the mean mass density of the immersion medium, k is the wave number and \bar{v}_s represents the velocity amplitude of the piston source at position $z = 0$. Eq. (1)

is also used in Ngaha et al.^{1,2,3,4} with applications for flow meters. The parabolic equation Eq. (1) remains valid under the assumption $(z/a)^3 \geq (ka)$ and for $ka \gg 1$, and requires the wave propagation to be in a narrow beam geometry.

For further analysis of Eq. (1), an integral solution based on the boundary condition above developed by Ngaha et al.^{1,2,3,4} by use of a two-dimensional spatial Fourier transformation in x and y coordinates is given by

$$q(\mathbf{x}) = \frac{k\rho_0 c}{2i\pi z} \cdot e^{ikz \frac{D_z^2}{2}} \int \int_B e^{\frac{ik((x-x_0)^2 + (y-y_0)^2)}{2z}} \cdot e^{-ikD_z(x-x_0)} \bar{v}_s(x_0, y_0) dx_0 dy_0, \quad (2)$$

where $D_z = \mathcal{M} \left(\frac{z}{2r} \right) \left(3 - \frac{z}{r} \right)$, $\mathcal{M} = v_{x,avg}/c$ is its flow Mach number, and $v_{x,avg}$ is the average flow velocity in the x -direction. It can be shown that $v_{x,avg} = \frac{2}{3}v_{x,max}$. For uniform flow where $v_{0x} = v_{x,max}$, Eq. (1) is reduced to an equation of the sound field through a uniform flowing fluid relying on the same boundary condition, and an integral solution of Eq. (1) can be found in Ngaha et al.^{1,2}.

From Eq. (2), the farfield approximation of the sound field generated by a uniform piston source through a laminar flow regime Eq. (1) developed in Ngaha et al.⁴ where $z \gg \frac{ka^2}{2}$ is expressed as follows

$$q(\mathbf{x}) \approx -i \frac{ka^2}{2} \frac{\rho_0 c \bar{v}_s}{z} \cdot e^{ikz \frac{D_z^2}{2}} \cdot e^{\frac{ik(x^2+y^2)}{2z}} \cdot e^{-ikD_z x} \cdot \frac{2J_1 \left((ka) \sqrt{(\tan \theta_x - D_z)^2 + \tan^2 \theta_y} \right)}{\left((ka) \sqrt{(\tan \theta_x - D_z)^2 + \tan^2 \theta_y} \right)}, \quad (3)$$

where $\tan \theta_x = \frac{x}{z}$ and $\tan \theta_y = \frac{y}{z}$. Further investigations based on numerical results are carried out below to illustrate Eqs. (1) and (2), based on the most influencing parameters on the sound field such as \mathcal{M} and ka -number, which also rely on inputs such as $v_{x,avg}$, k , c , a or frequency f .

3 NUMERICAL SIMULATION

Simulations of Eqs. (2) and (3) rely on input parameters of relevance for underwater acoustic applications over a short distance described in the introduction. For sound propagating in open water, we consider current velocities up to 5 m/s over small distance of $z_{max} = 10$ m, and a speed of sound c of 1500 m/s. The frequency of ultrasonic waves in echo sounders is typically in the order of 15 kHz to 300 kHz, we consider the maximal frequency of $f = 300$ kHz. Numerical simulations based on these inputs will be compared to the ones in natural gas pipe flow and water pipe flow, relying on typical fluid industry set-up. For generality, we especially extend the pipe diameter to $d = z_{max} = 10$ m, to visualize the wave in the farfield region. In pipe flow, a speed of sound of $c = 400$ m/s for natural gas, and $c = 1500$ m/s for water have been taken. Flow velocities $v_{x,avg}$ up to 40 m/s for natural gas, and 15 m/s for water are applied.

Calculations are carried out at frequencies of 500 kHz for pipe flow of natural gas, and 2 MHz for pipe flow of water. For both underwater and for the different pipe flows, $ka = 60$ is used. This corresponds to the uniform piston radius $a = 0.048$ m in the ocean, $a = 0.0076$ m in gas pipe flow, and $a = 0.0071$ m in water pipe flow, respectively. For the acoustic wave, both the amplitude and phase are depicted along the transducer axis in the x, z system ($y = 0$) until it reaches the straight opposite side at the endpoint z_{max} . Plots are only displayed when $L = a(ka)^{(1/3)} \leq z \leq z_{max} = 2r$. L , L_2 and L_3 are the minimal distances where the parabolic equation remains valid and R , R_2 and R_3 represent the Rayleigh distance indicated by the pink vertical dashed line for each case. r is indicated by the dark vertical dashed line.

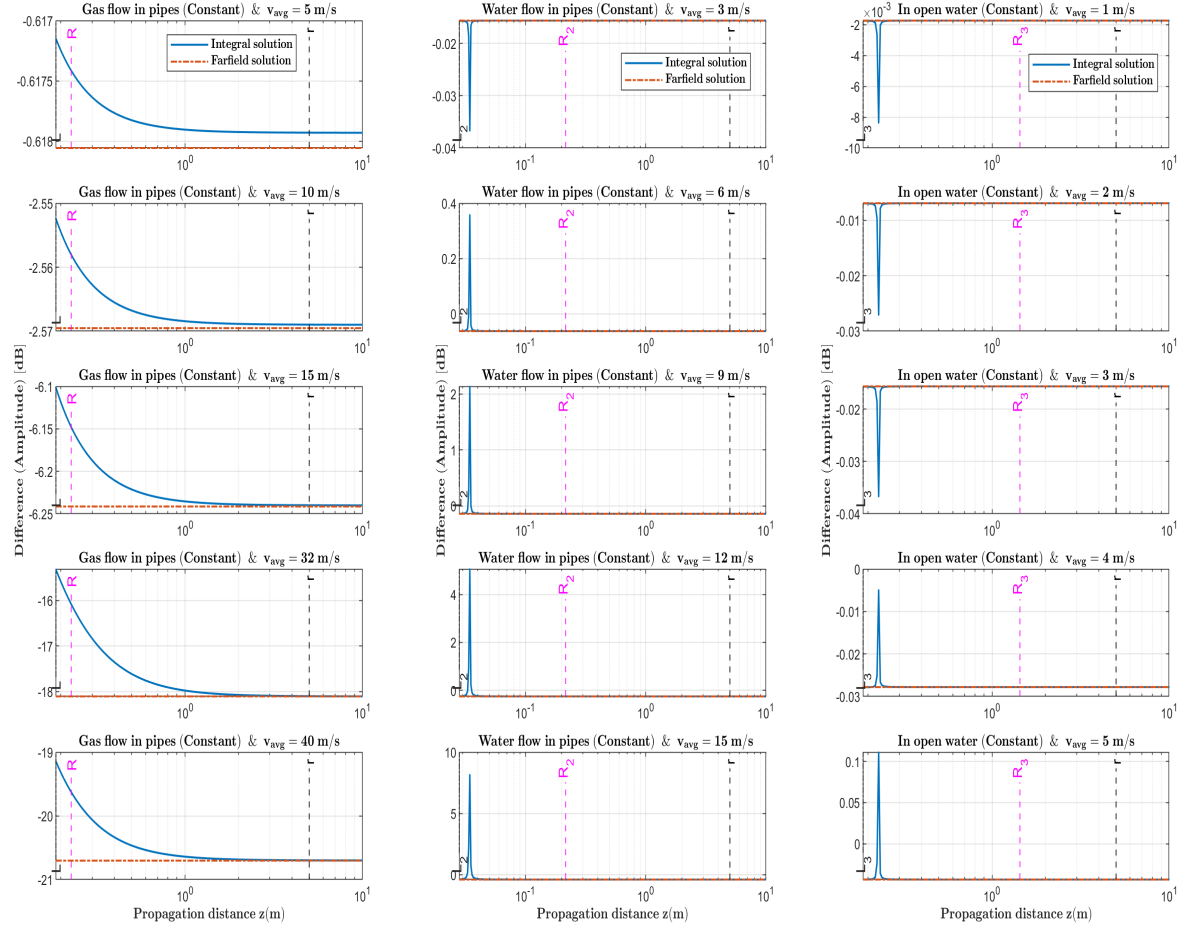


Figure 1: Amplitude ratio ($20 \log_{10} [Q(z)]$) between the acoustic field at constant flowing and no-flowing conditions along the transducer axis (at $x = 0$), for $ka = 60$ and for different flow velocities. Gas flow in pipes (column 1), water flow in pipes (column 2), and in open water (column 3).

The integral solution Eq. (2) is calculated by use of the Riemann summation method. Note that for a steady representation of the acoustic wave in the farfield, we take out rapid phases under exponential forms from both Eqs. (2) and (3). The phase in the farfield of a transmitting transducer is therefore relative to the corresponding spherical wave. We set $Q(z) = |q(z)/q_{ref}(z)|$ as being the amplitude of the sound pressure under flowing conditions that has been normalized to the amplitude of the pressure at no-flow conditions ($q_{ref}(z)$), and $H(z) = \angle [q(z)/(q_{ref}(z)(\rho_0 c \bar{v}_s))]$ is the difference in slow phases between under flowing and no-flow conditions.

Plots in Figs. 1 to 4 are illustrated along the transducer axis (at $x = 0$) as a function of propagation distance z for $ka = 60$, by use of the integral solution indicated by the blue line and the farfield approximation by the red dashed line. A set of average flow velocities $v_{avg} = 5$ m/s, 10 m/s, 15 m/s, 32 m/s, and 40 m/s is considered for gas flow in pipes (column 1). For water flow in pipes (column 2), we have $v_{avg} = 3$ m/s, 6 m/s, 9 m/s, 12 m/s, and 15 m/s and in open water (column 3), we have $v_{avg} = 1$ m/s, 2 m/s, 3 m/s, 4 m/s, and 5 m/s.

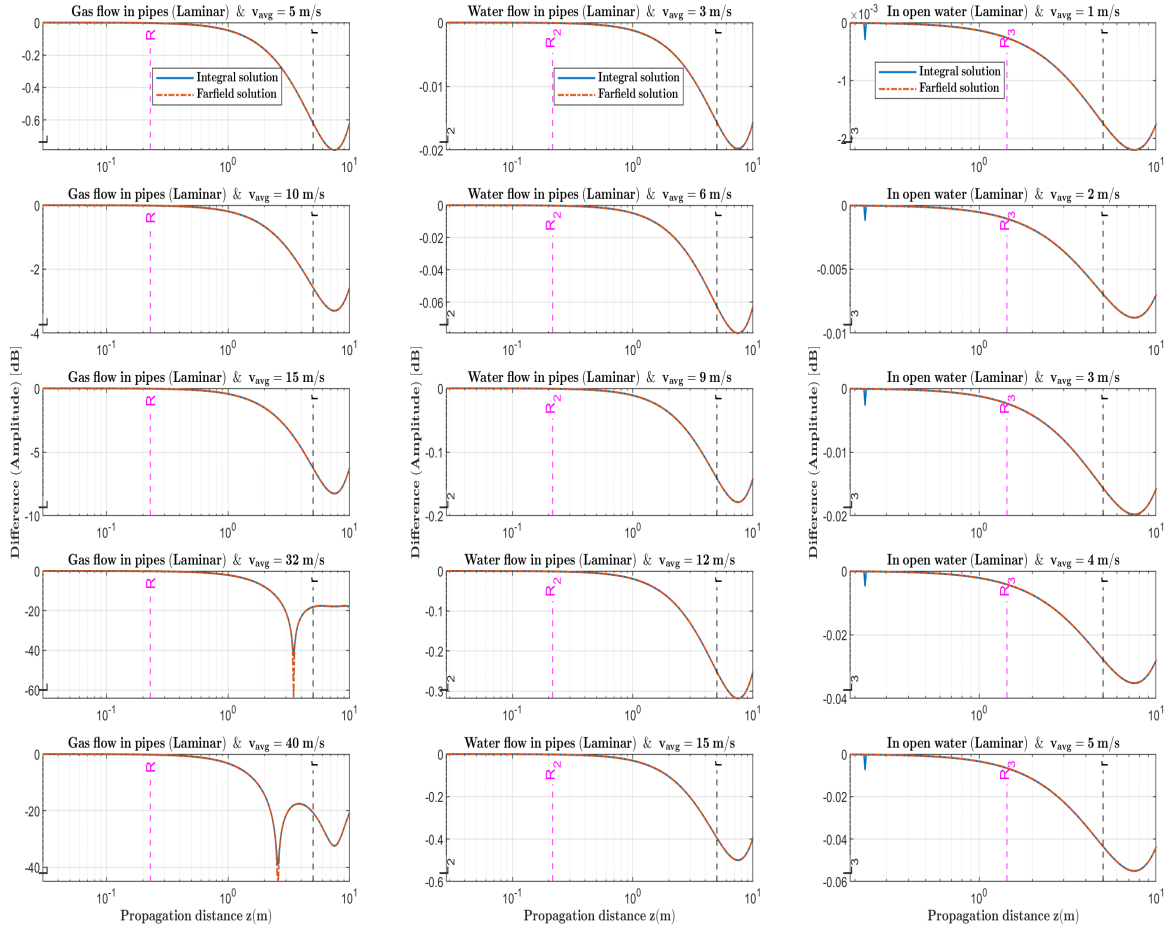


Figure 2: Amplitude ratio ($20 \log_{10} [Q(z)]$) between the acoustic field at laminar flowing and no-flowing conditions along the transducer axis (at $x = 0$), for $ka = 60$ and for different flow velocities. Gas flow in pipes (column 1), water flow in pipes (column 2), and in open water (column 3).

Figures 1 and 2 show amplitudes of the sound pressure under flowing conditions including ocean currents in open water (both for uniform (Fig. 1) and laminar (Fig. 2) flow cases) relative to the amplitude of the sound at no-flow conditions, and Figs. 3 and 4 represent the difference in slow phases between the slow phase under flowing conditions compared with the slow phase at the no-flow condition.

For uniform gas and water flows in pipes (column 1 and 2 in Fig. 1), a fair correspondance in the amplitude is observed between the integral and farfield solutions close to the Rayleigh distance and beyond. However, for the integral solution and for flow velocities of 32 m/s and 40 m/s for gas flow in pipes, an average difference of 2 dB is seen compared to the farfield solution. For water flow in pipes, a peak in the amplitude of the integral solution from 2 to 10 dB is also observed compared to the farfield solution for flow velocities of 9 m/s, 12 m/s, and 15 m/s respectively. We remark that the flow velocity effect remains almost insignificant on the amplitude under uniform gas and water flow in pipes for these flow velocities.

For laminar gas and water flows in pipes (column 1 and 2 in Fig. 2), a good agreement in the amplitude is observed between integral and farfield solutions for all flow velocities. An oscillation in the farfield is

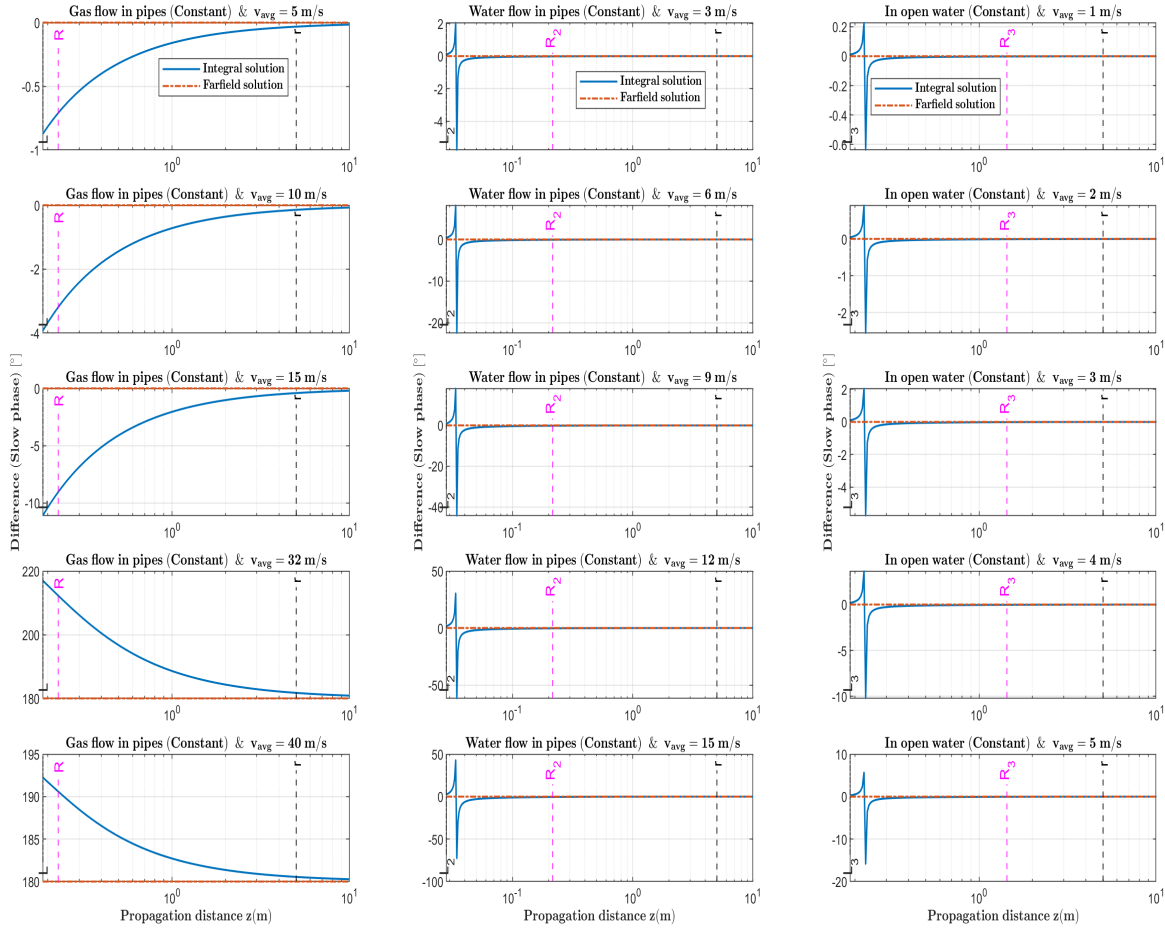


Figure 3: Slow phase difference ($H(z)$, $^{\circ}$) between the acoustic field at constant flowing and no-flowing conditions along the transducer axis (at $x = 0$), for $ka = 60$ and for different flow velocities. Gas flow in pipes (column 1), water flow in pipes (column 2), and in open water (column 3).

seen at mid distance where the flow velocity reaches its maximum. In the nearfield, we can see that the flow effect is insignificant on the amplitude for laminar gas flow in pipes due to the no-slip condition^{3,4}. However, in the farfield, the flow effect gets significant for laminar gas flow in pipes for flow velocities from 15 m/s to 40 m/s (column 1, Fig. 2), but remains negligible for water flow in pipes.

In open water (column 3, Figs. 1 and 2), a good agreement in the amplitude is observed between integral and farfield plots for both flow profiles. In the nearfield, a last maximum in the amplitude of the integral solution is also seen under uniform flow cases, and a last minimum in the farfield is observed for integral and farfield solutions under laminar flow profiles and for the different flow velocities. However, the flow effects remains insignificant for both flow profiles due to low flow velocities compared to the gas and water flow in pipes where high flow velocities are used.

For slow phases over the propagation distance (Figs. 3 and 4), and for uniform gas flow in pipes (column 1, Fig. 3), no close agreement is observed between integral and farfield solutions with increasing flow velocity. For the laminar flow profile (column 1, Fig. 4), there is a fair correspondence in the slow phase

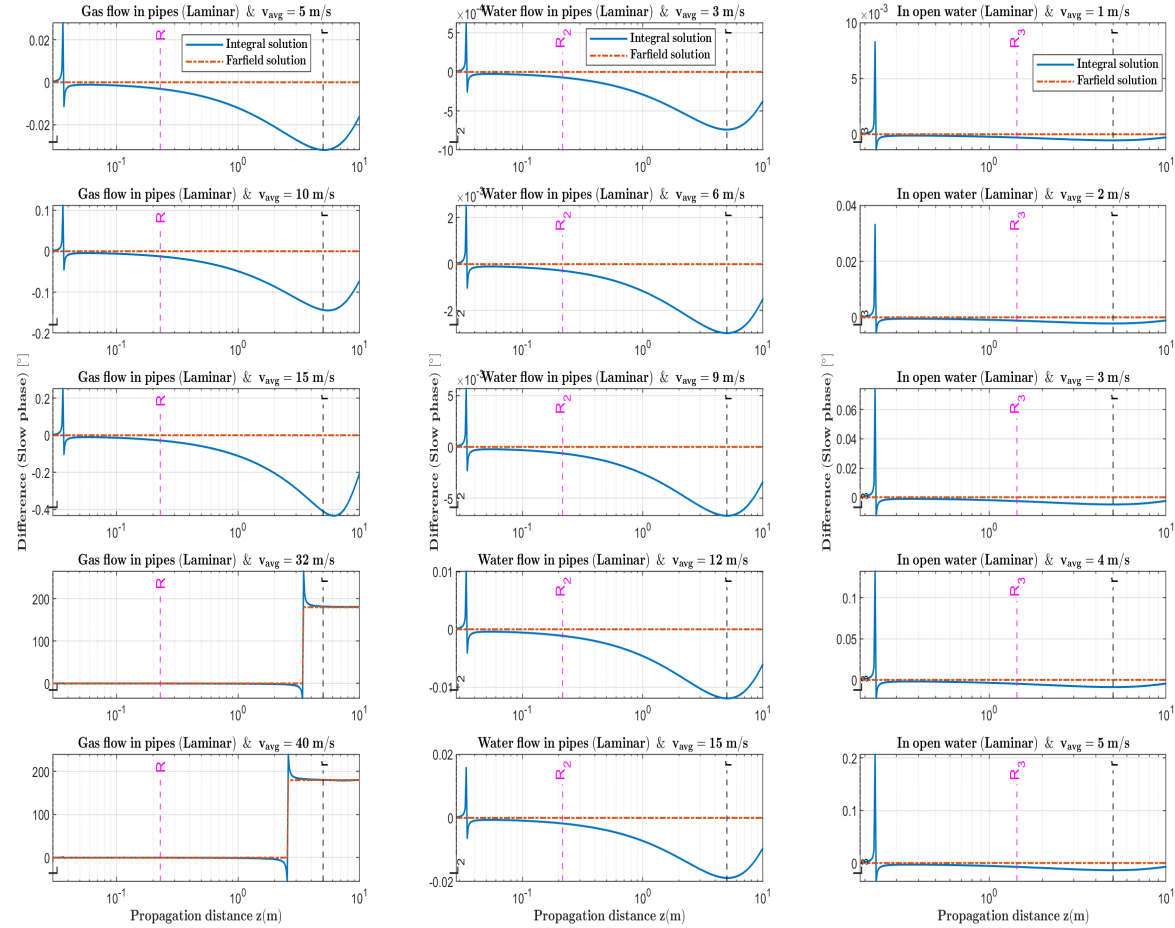


Figure 4: Slow phase difference ($H(z)$, $^{\circ}$) between the acoustic field at laminar flowing and no-flowing conditions along the transducer axis (at $x = 0$), for $ka = 60$ and for different flow velocities. Gas flow in pipes (column 1), water flow in pipes (column 2), and in open water (column 3).

between the two solutions, for the different flow velocities.

For integral solution (column 1, Fig. 4), the slow phase exhibits a last extrema due to the maximum laminar flow velocity when approaching the mid propagation distance along z . For integral and farfield solutions in both flow profiles, the higher the flow velocities, the more the gap between the slow phase under flowing and no-flow conditions gets significant.

For water flow in pipes (column 2, Figs. 3 and 4), and in open water (column 3, Figs. 3 and 4), a good agreement between integral and farfield solutions is seen. However, a last extrema in the nearfield is observed for the integral solution, for the different flow velocities. For uniform flow case (column 2, Fig. 3), this extrema remains significant with increasing flow velocity. For laminar flow case (column 2, Fig. 4) and in the farfield, there is a last minimum in the slow phase of the integral solution, where the laminar flow velocity reaches its maximum approaching the mid propagation distance along z . Therefore, for water flow in pipes and in open water, flow effects are insignificant on slow phases and remains negligible under the two flow profiles. Note that the farfield solution remains just an idealized representation of the

acoustic wave in the farfield.

4 CONCLUSION

In this work, a theoretical study of whether flow effects on a sound field over a small range distance can be important to take into account for underwater acoustic applications has been carried out, by use of a parabolic wave equation. This also includes diffraction effects on sound beams. We have computed acoustic waves through a uniform and a laminar flowing fluid in open water by use of integral and farfield solutions. The sound source is a uniform piston source located in a flat baffle. The flow direction is perpendicular to the sound propagating over a short propagation distance of 10 m. Numerical simulations are presented under different flow velocities for $ka = 60$, and are compared to the ones in natural gas pipe flow and water pipe flow, based on industry set-up. As results, the acoustic diffraction correction effect depends on the path length, the ka number and the flow velocity, as expected. Results here also indicate that for uniform and laminar gas flow in pipe, flow effects on acoustic waves get significant with increasing flow velocities. However, for water flow in pipes and in open water, flow effects over a short range distance are insignificant on sound waves and remain negligible under the two flow profiles, and for the different flow velocities considered.

REFERENCES

1. D. Tchatat and K-E. Frøysa, "Parabolic equation simulation of a sound beam propagating through a flowing fluid", *Proceedings of the 45th Scandinavian Symposium on Physical Acoustics, Online*, Norway (2022).
2. D. T. Ngaha and K-E. Frøysa, "Parabolic equation simulation of diffraction effects in a sound beam propagating through a flowing fluid". *Proc. Mtgs. Acoust.* **51**(1), Chicago (2023).
3. D. T. Ngaha and K-E. Frøysa, "Diffraction effects for acoustic beams propagating through a laminar flowing fluid". *to submit*, (2024).
4. D. T. Ngaha and K. E. Frøysa, "Far-field of acoustic beams in a flowing fluid". *to submit*, (2024).
5. A. S. Khimunin, "Numerical calculation of the diffraction corrections for the precise measurement of ultrasonic absorption", *Acustica*, **27**(4) 173-181 (1972).
6. A. S. Khimunin, "Numerical calculation of the diffraction corrections for the precise measurement of ultrasound phase velocity", *Acustica*, **32** 192-200 (1975).
7. H. Seki, A. Granato, and R. Truell, "Diffraction Effects in the Ultrasonic Field of a Piston Source and Their Importance in the Accurate Measurement of Attenuation", *J. Acoust. Soc. Am.* **28**(2) 230-238 (1930).
8. L. Brekhovskikh and Y. Lysanov, *Fundamentals of Ocean Acoustics*, Springer-Verlag (1982).
9. W. S. Burdic, *Underwater acoustic system analysis*, Prentice Hall (1984).
10. J. MacDonald, H. Ghannadrezaii, J. -F. Bousquet and D. Barclay, "Analysis of the Impact of Flow on the Underwater Acoustic Channel", *OCEANS 2021: San Diego-Porto*, San Diego, CA, USA, 1-8 (2021).
11. Y. B. Kaya and M. Ranjbar, "A Review on Methods and Approaches in Underwater Acoustics", *Computational Research Progress in Applied Science & Engineering, CRPASE: Transactions of Applied Sciences* **6** 220-227 (2020).
12. A. D. Pierce, "Wave equation for sound in fluids with unsteady inhomogeneous flow", *J. Acoust. Soc. Am.*, **87**(6) 2292-2299 (1990).
13. V.E. Ostashev and D.K. Wilson, *Acoustics in Moving Inhomogeneous Media (2nd ed.)*, CRC Press (2015).